Theoretical plasma distributions consistent with Ulysses magnetic field observations in a high-speed solar wind tangential discontinuity

J, De Keyser, M. Roth and J. Lemaire
Belgian Institute for Space Aeronomy, Brussels, Belgium

B. T. Tsurutani and C. M. Ho
Jet Propulsion Laboratory, California institute of Technology, Pasadena, California

C. M. Hammond
Los Alamos National Laboratory, Los Alamos, New Mexico

Received _ –.. . --.-. _.__..- ---- .——; accepted ---- .._—_ . . . .

To appear in Geophysical Research *Letters*, 1995.

Short title: PLASMA DIS'IWBUTIONS IN TANGENTIAL DISCONTINUITIES

Abstract. The overall multi-layer structure of the magnetic field profile observed by ULYSSES across a broad solar wind tangential discontinuity can be reproduced fairly well by means of a kinetic model. Such a simulation provides complementary information about the velocity distribution functions, which are not always known due to the low time resolution inherent in plasma measurements. The success of such a simulation proves that our kinetic model can be used as a realistic basis for further studies of the structure and stability of tangential discontinuities.

Introduction

Tangential discontinuities (TDs) are a prevalent feature of the solar wind (see e.g. [*Burlaga et al.*, 1977]). Results from ULYSSES indicate that TDs are common also at high heliographic latitudes [*Tsurutani et al.*, 1994]. Solar wind TDs often exhibit different characteristic scales and are associated with shears in both the magnetic field and plasma velocity. A prerequisite for any theoretical study of TDs is a realistic model that is able to account for the overall internal structure observed in high time resolution magnetic field measurements, Kinetic TD models based on Vlasov equilibria (e.g. [*Lemaire and Burlaga*, 1976; *Lee* and *Kan*, 1979; *Roth et al.*, 1993; *Kuznetsova et al.*, 1994; *Kuznetsova and Roth, 1995]) differ* from each other by the analytical form of the velocity distribution function (VDF). They cannot account for the complex multiscale nature often present in solar wind TDs, as the number of free parameters in these models is reduced to a minimum (like in *Roth et al.* [1993] or *Kuznetsova* and *Roth* [1995]) depending on the specific application. In this paper a generalized model (that includes most previous models as special cases) using several species and parameterized VDFs is shown to be powerful enough to explain the overall magnetic field variation across a solar wind TD observed by ULYSSES. In the absence of plasma data with sufficient time resolution, such a simulation gives us some clues about the actual VDFs. The aim of this paper is not the study of this particular solar wind TD; rather, the emphasis is on the applicability of the model and its suitability as a basis for further theoretical investigation.

The kinetic TD model

The standard procedure for solving the Vlasov equations for charged particles (mass m and charge Ze) moving in a steady plane TD electromagnetic configuration (see e.g. [*Longmire*, 1963], chapter 5) consists of first expressing the single-valued VDFs in terms of the constants of motion: the particle's energy H and canonical momenta p_y and p_z (x being the normal to the TD-plane). In a second phase, the partial densities and currents are obtained as functions of the electrostatic potential $\phi(x)$ and the vector potential components $a_y(x)$ and $a_z(x)$, by integrating the VDFs over velocity space. Finally, Maxwell's equations lead to a set of coupled ordinary differential equations for $a_y(x)$ and $a_z(x)$, supplemented by the quasi-neutrality condition. This set is solved numerically.

The VDF used here is:

$$F = \eta(H, p_y, p_z) G(U_y(p_y), U_z(p_z)),$$

where η is a maxwellian at temperature T, shifted around an average tangential velocity' V:

$$\eta = N\left(\frac{m}{2\pi T}\right)^{\frac{3}{2}} \exp\left(-\frac{H}{T} - \frac{mV^2}{2T} + \frac{p_y V_y + p_z V_z}{T}\right)$$

and G is a cutoff function ($C_i \geq 0; i = 1, \ldots 4$)

$$G = [C_1 \operatorname{erfc}(U_y)\operatorname{erfc}(-U_z) + C_2 \operatorname{erfc}(-U_y)\operatorname{erfc}(-U_z) + C_3 \operatorname{erfc}(U_y)\operatorname{erfc}(U_z) + C_4 \operatorname{erfc}(-U_y)\operatorname{erfc}(U_z)]/4$$

with $U_{y,z} = (p_{y,z} - mV_{y,z} - hp_{0y,z})/ZeB_0\rho\sqrt{l_{y,z}^2 + 1}$, where $\rho = \sqrt{2mT}/|Z|eB_0$ is the gyroradius of the particle ill a reference magnetic field B_0, and $h = \operatorname{sign} Z$. The cutoff function depends on the transition lengths l_y and 1, (≥ 1), the constants C_i (defining the forbidden phase space quadrants), and p_{0y} anti p_{0z} (overlap of the occupied phase space quadrants). It may be used to express the fact that charged particles from one side cannot penetrate much into the other half space, or to describe particle populations that exist only inside the transition layer (like, e.g., in the Harris model [*Harris*, 1962]).

Observations and simulation

Amongst the many TDs observed by ULYSSES we have selected one, observed on July 3, 1993, 5:29 UT, at 4.57 AU and -33.8° heliographic latitude. Dashed lines on figure 1 show the magnetic field components in the minimum variance frame. The spacecraft velocity with respect to the Sun (a few km/s) is negligible in comparison to the high speed of the solar wind. MVF orientation and velocity data show the normal speed of ULYSSES relative to : he TD plane to be 750 ± 10 km/s, implying a width of about 130000 km. This exceptional width (230 gyroradii of 21.5 eV protons in a 0.85 nT field) and the multiscale magnetic field variations indicate that this transition is composed of several current sheets. Solar wind TDs are known to have an average width of 36 ± 5 gyroradii [*Lepping and Behannon*, 1986], placing this particular TD among the widest ones.

We distinguish three parts in the magnetic field magnitude dip: the left and right inner regions (IL and IR, see figure 1) anti a central inner depression (IC). The dip is bounded by two outer regions (OL and OR) defining the solar wind environment. Figure 1 shows that the transition consists of a B_z reversal, while B_y remains essentiality constant; the magnetic field rotates over 90.6°. According to *Kuznetsova and Roth [1995]*, such a large rotation requires the presence of inner particle populations [*Harris*, 1962], i.e., populations with a density that decays rapidly with distance from the center of the transition,

The simulation relies on the high time resolution magnetometer data (1 vector/s), and plasma data from the ion spectrometer (returning 3-dimensional spectra every 4 to 8 minutes) and the electron

instrument (returning either 2- or 3-dimensional spectra every 5 to 11 minutes). Only solar wind properties near the right edge of the transition are available; there are no data close to the left edge, nor inside the transition. Because of the symmetry in magnetic field intensity on both sides of the TD, it is reasonable to take equal plasma densities and temperatures for the outer regions. We also assume that the velocity shear between both outer plasmas can be neglected

Table 1 gives the values of the VDF parameters that are able to account fairly well for the observed magnetic field profile, We have introduced 5 sets of populations, Each set consists of electrons of 4.4 eV, a proton population of '21.5 eV, and 100.0 eV alpha particles (the latter contribute significantly to the total current). For the outer populations we have used the plasma data. We have assumed an overlap between the outer populations (see figure 2) defining a central plasma density enhancement of 12 %. This explains the central inner field depression. To reproduce the asymmetry in the B_y component observed in the left and right inner depressions, we have used different z bulk velocities for the left and right inner populations. These inner populations also contribute to the B_z reversal through their drift velocities along y. 'To improve the fit even more, we have added a wide central inner population set. The electron densities, shown in figure 2, illustrate the role of the populations in each region.

Figure 1 compares the simulated magnetic field (solid lines) with the observations (dashed lines), showing the good fit of the overall magnetic field profile. The fine wavy-like structure superimposed on it cannot be reproduced. It may be ascribed to the propagation of waves across the TD. Alternatively, the TD might be in a state of turbulence [*Kuznetsova et al., 1995*]. Nevertheless, equilibrium models are a first approximation; they can be used to describe the unperturbed state in a subsequent study of TD instabilities.

Discussion

In this paper we have used a generalized Vlasov model of TDs. We have obtained a "best choice" for the VDF parameters that mimics a TD magnetic field profile recorded by ULYSSES. Previously, only hypothetical solar wind TDs have been simulated with Vlasov models [*Lemaire and Burlaga*, 1976; *Roth, 1986*]; here, we model an actually observed event. in the absence of high time resolution plasma data, the simulation gives important clues about the nature of the actual VDFs. For instance, inner populations with different bulk velocities have to be postulated to account for the observed magnetic field rotation. The multi-layer structure of the transition is controlled by the length scales and separation (or overlap) of the populations.

The TD simulated here is quite large and represents a piling up of several current layers: it is a

denser plasma region, separated from the surrounding solar wind by a current sheet on either side (with current densities of the order of 3.10^{11} A/m^2). In general, simulations like the one performed here, offer the possibility of computing quantities which are not directly observable, such as the electric field strength. For instance, in this particular simulation we have obtained electrostatic potential variations of less than 50 mV, corresponding to an extremely weak *electric* field along the TD normal. Its precise value is of no particular interest; what matters is that an equilibrium electric field exists as a natural consequence of the tendency of a plasma to remain neutral, Still, it plays an important role in the study of magnetic field line stochasticity and particle diffusion in electrostatically non-equipotential TDs [*Kuznetsova and Roth, 1995].*

The successful simulation demonstrates the ability of the kinetic model to describe the overall characteristics of observed magnetic field profiles. Therefore, it can serve as a basic model for further studies of TD related phenomena. For instance, the wave-like structure of the small-scale magnetic field variations can be analyzed by looking at the difference between the equilibrium model and the high resolution observations. The power spectrum of the difference can provide insight into possibly excited instabilities and their preferred wavelengths.

A number of problems associated with the one-dimensional, time-independent Vlasov approach should be kept in mind. In particular, Vlasov theories of plane TDs employ nonunique distribution functions and do not address the problem of particle accessibility [*Whipple et al.*, 1984]. Moreover, current layers with large magnetic or velocity shear, density and temperature gradients, are thermodynamically nonequilibrium systems that have an excess of free energy and are potentially unstable with respect to the excitation of large scale electromagnetic perturbations [*Kuznetsova et al.*, 1995]. Therefore, TDs most likely are in a state of turbulence rather than in a state of equilibrium. *Kuznetsova et al. [1995] have* proposed a method which reduces the arbitrariness in the Vlasov formulation: the optimal choice for the free parameters of the model is the one leading to the most stable configuration that satisfies the boundary conditions.

In order to study the time evolution of TDs, one can adopt a realistic ID equilibrium model, like the one presented here, as an initial state, and consider the effects of superposed perturbations. This introduces 3D effects in the model in the form of small-amplitude long-wavelength variations of fields in the plane of the current sheet. As an alternative, hybrid particle simulations that use an ensemble of ion particles immersed in an electron fluid (e. g., [*Cargill* and *Eastman*, 1991; *Omidi and Winske*, 1995]) can trace the evolution of TDs. Electron inertia, however, plays a critical role in configurations with large magnetic shear and cannot be adequately described by present particle simulation codes,

Acknowledgments. The authors thank A. Balogh (Imperial College, London, England) for providing the magnetic field data, and J. L. Phillips (Los Alamos National Laboratory, NM) for the plasma data. They also thank M. M. Kuznetsova for fruitful discussions. J. D. K., M. R. and J. L. are supported by the ESA (PRODEX) project "Interdisciplinary Study of Directional Discontinuities" as part of the ULYSSES mission, and acknowledge the support of the Belgian Federal Services for Scientific, Technological and Cultural Affairs.

References

Burlaga, L. F., J. F. Lemaire, and J.M. Turner, Interplanetary currents sheets at 1 AU, *J. Geophys. Res., 82,* 3191, 1977.

Cargill, P.J., and T.E. Eastman, The structure o f tangential discontinuities. 1. Results of hybrid simulations, *J. Geophys. Res.,* 96, 763, 1991.

Harris, E. G., On a plasma sheath separating regions of oppositely directed magnetic field, *Nuovo Cimento, 23,* 115, 1962.

Kuznetsova, M. M., M. Roth, Z. Wang, and M Ashour-Abdalla, Effect of the relative fEow velocity on the structure and stability of the magnetopause current layer, *J. Geophys. Res., 99,* 4095, 1994.

Kuznetsova, M. M., M. Roth, and L.M. Zelenyi, Kinetic structure of the magnetopause: equilibrium and percolation, in *Physics of the magnetopause,* edited by B. U Ö Sonnerup, M. Thomsen, anti P. Song, AGU, Washington, D. C., 1995, in press.

Kuznetsova, M. M., and M. Roth, Thresholds for magnetic percolation through the magnetopause current layer in asymmetrical magnetic fields, *J. Geophys. Res., 100,* 155, 1995.

Lee, L. C., and J.R. Kan, A unified kinetic model of the tangential magnetopause structure, *J. Geophys. Res.,* 84, 6417, 1979.

Lemaire, J. and L.F. Burlaga, Diamagnetic boundary layers: a kinetic theory, *Astr ophys. Space Sci.,* 45, 303, 1976.

Lepping, R.P. and K.W. Behannon, Magnetic field directional discontinuities: characteristics between 0.46 and 1.0 AU, *J. Geophys. Res.,* 91, 8725 -S741, 1986.

Longmire, C.L., *Elementary plasma physics,* Interscience Publishers, New York, 1963.

Omidi, N. and D. Winske, Structure of the magnetopause inferred from one. dimensionally hybrid simulations, *J. Geophys. Res., 100,,* 11935, 1995.

Roth, M., A computer simulation study of the microscopic structure of a typical current sheet in the solar wind, in *The Sun and the Heliosphere in Three Dimensions, ASSL123,* edited by R.G. Marsden, I), Reidel Publ. Co., Dordrecht) pp. 167-171, 1986,

Roth, M., D.S. Evans, and J. I,. Lemaire, Theoretical structure of a magnetospheric plasma boundary: application to the formation of discrete auroral arcs, *J. Geophys. Res, 98,,* 411, 1993.

Tsurutani, B. T., C.M. Ho, E.J. Smith, M, Neugebauer, B E. Goldstein, J.S. Mok, J.K. Arballo, A, Balogh, D.J. Southwood, and W.C. Feldman, The relationship between interplanetary discontinuities and Alfvén waves: Ulysses observations, *Geophys. Res. Lett., 21,* 2267-2270, 1994.

Whipple, E. C., J. R. Hill, and J. D. Nichols, Magnetopause structure and the question of accessibility, *J. Geophys. Res.,* 89, 1508-1516, 1984.

This manuscript was, prepared with the AGU LaTeX macros v3. 1

Table 1. Plasma populations used in the simulation

population	Z	m/m_p	$N(\mathrm{cm}^3)$	$T(eV)$	(V_y, V_z) (km/s)	(C_1, C_2, C_3, C_4)	$(l_y^*, l_z^*)^a$	$(p_{0y}^*, p_{0z}^*)^b$
	-1	0.00055	0.3348	4.4	(0,0)	**(0,0,1,1)**	(-,11)	*(-,1.2)*
outer left	+1	1.00	0.301s	21.5	(0,0)	**(0,0,1,1)**	(-,11)	*(-,1.2)*
(OL) ,	+2	*3.97*	0.0165	100.0	(0,0)	(0,0,1,1)	(-,11)	(-,1.2)
	-1	0.00055	0.1540	4.4	(0.25,-0.34)	(0,0,1,1)	(-,4.5)	(-,-15)
inner left	+1	1.00	0.1400	21.5	(-1.22, 1 66)	(0,0,1,1)	(-,45)	(-,-15)
(IL)	+2	*3.97*	0.0070	100.0	(-5.68, 7.73)	(0,0,1,1)	(-,4.5)	(-,-15)
	-1	0.00055	0.0066	4.4	(025. o)	(1,1,1,1)	(-,-)	(-,-)
inner center	+1	1.00	0.0060	21.5	(-1.22, o)	(1,1,1)1)	(-,-)	(-)-)
(It)	-12	3.97	0.0003	100.0	(-568, O)	(1,1,1,1)	(-,-)	(-,-)
	-1	0.00055	0.0550	4.4	(0.25, 0.10)	(1,1,0,0)	(-,4,0)	(-,14)
inner right	+1	1.00	0.0500	21.5	(-1.22,-049)	(1,1,0,0)	(-,4.0)	(-,14)
(IR)	+2	3.97	0.0025	100.0	(-5.68, -?.27)	(1,1,0,0)	(-,4,0)	(-,14)
	-1	0.00055	0.3348	4.4	(0.0)	(1,1,0,0)	(-,11)	(-,-1.2)
outer right	+1	1.00	0.3018	21.5	(0,0)	(1,1,0,0)	(-,11)	(-,-1,2)
(OR)	+2	3.97	0.0165	100.0	(0,0)	(1,1,0,0)	(-,11)	(-,.1.2)

[a] $l_{y,z}^* = l_{y,z}\rho/\rho_0$ where ρ_0 is the thermal gyroradius of a 20 eV proton in a 1 nT magnetic field (650 km)

[b] $p_{0y,z}^* = p_{0y,z}/p_0$ where p_0 is the thermal momentum of a 20 eV proton (10^{-22} kg.m/s)

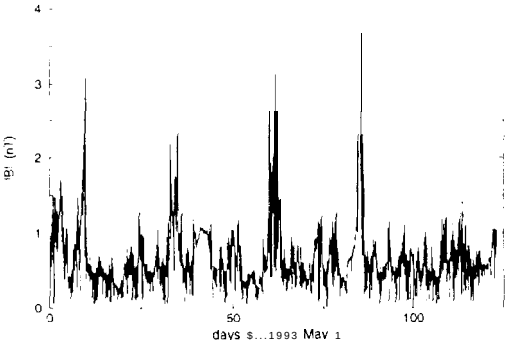

Figure 1. Ulysses magnetic field data for 1993, May-August. The plasma cloud under study was observed on day 63, at the end of the third CIR encounter.

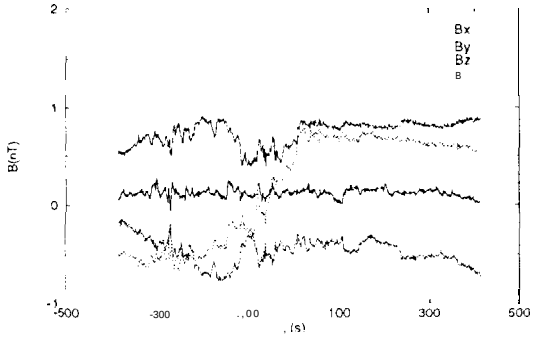

Figure 2. High-resolution MVF magnetic field. Time is given relative to July 3, $5^h\ 30^m$

Table 1, Plasma populations used in the simulation

population	Z	m/m_p	$N(\mathrm{cm}^3)$	$T(\mathrm{eV})$	(V_y, V_z) (km/s)	(C_1, C_2, C_3, C_4)	$(l_y, l_z)^a$	$(p_{0y}, p_{0z})^a$
	-1	0.00055	0.3348	4.4	**(0,0)**	(0,0,1,1)	(-)11)	(-,1.2)
outer left	+1	1,00	0.3018	21.5	(0,0)	(0,0,1,1)	(-,11)	(-,1,2)
	+2	3.97	0.0165	100.0	(0,0)	(0,0,1,1)	(-,11)	(-,1,2)
	-1	0.00055	0.1540	4.4	(0.25, -0.34)	(0,0,1,1)	(-,4.5)	(-,-15)
inner left	+1	1.00	0.1400	21.5	(-1.22, 1.66)	(0,0,1,1)	(-,4.5)	(-,-15)
	+2	3.97	0.0070	100.0	(-5,68, 7.73)	(0,0,1,1)	(-,4,5)	(-,-15)
	-1	0.00055	0.0066	4.4	(0.25, O)	(1,1,1,1)	(-,-)	(-,-)
inner center	+1	1.00	0.0060	21.5	(-1,22, o)	(1,1,1,1)	(-,-)	(-,-)
	+2	3.97	0.0003	100.0	(-5.68, o)	(1,1,1,1)	(-,-)	(-,-)
	-1	0.00055	0.0550	4.4	(0.25, 0.10)	(1,1,0,0)	(-,.4.0)	(-,14)
inner right	+1	1.00	0.0500	21.5	(-1,22, -0.49)	(1,1,0.0)	(-,4,0)	(-,14)
	+2	3.97	0.0025	100.0	(-5.68, -2.27)	(1,1,0,0)	(-,4.0)	(-,14)
	-1	0.00055	0.3348	4.4	(0.0)	(1,1,0,0)	(-,11)	(-,-1,2)
outer right	+1	1,00	0.3018	21.5	(0.0)	(1.1,0,0)	(-,11)	(-.-1,2)
	+2	3.97	0.0165	100.0	(0,0)	(1,1,0,0)	(-,11)	(-,-1 .2)

[a] The characteristic lengths are given relative to the gyroradius of a 20 eV proton in a 1 nT magnetic field; the overlap parameters are relative to the momentum of a thermal proton.

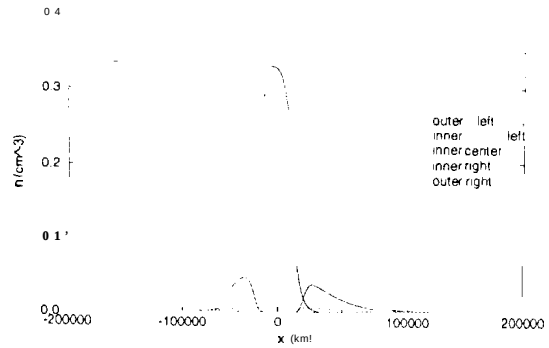

Figure 3. Electron number densities

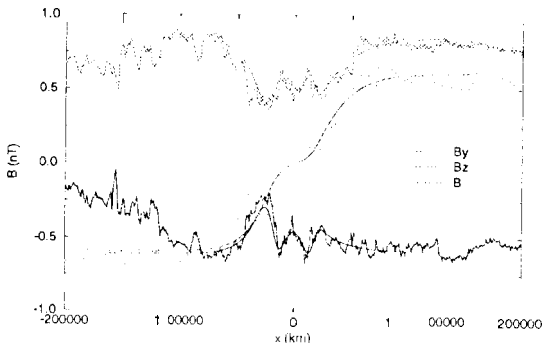

Figure 4. Observed and simulated magnetic field

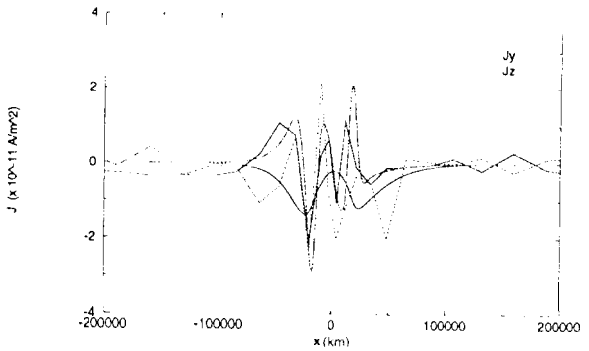

Figure 5. Comparison of the currents computed from magnetic field data with the simulated ones